



TURBOMACHINERY & PUMP SYMPOSIA | VIRTUAL  
**DECEMBER 8-10, 2020**  
SHORT COURSES: DECEMBER 7, 2020

## DRY GAS SEAL MATERIAL INVESTIGATION FOR ENHANCED SLOW ROLL & WINDMILLING RELIABILITY

**Dr. Christina Twist**  
Manager, Gas Seals R&D  
John Crane  
Morton Grove, Illinois, USA

**Dr. Jiao Yang**  
Product Manager  
John Crane  
Slough, United Kingdom

**Kanza Amanullah**  
Senior Engineer, Gas Seals R&D  
John Crane  
Slough, United Kingdom

**Marwan Jahchan**  
Global Dry Gas Seal Manager - Geo Markets  
John Crane  
Slough, United Kingdom

**Ian Goldswain**  
Director, Gas Seals R&D  
John Crane  
Slough, United Kingdom



*Dr. Christina Twist is a manager within the Gas Seals R&D division at John Crane. She received her Ph.D. from Northwestern University (2013) with a specialty in tribology and a B.S. from Texas A&M University (2007).*



*Dr. Jiao Yang is a product manager at John Crane and is currently located in Slough, UK. She holds a Ph.D. in Materials Science from Ecole Centrale de Lyon in France. She started her job as a materials engineer in John Crane China, then relocated to John Crane UK as a product manager. Her research is mainly focused on the tribological behavior of coatings in various environments. Her current responsibility is management of the seal product portfolio and providing support to new product development.*



*Kanza Amanullah is a Mechanical Engineer graduate of Brunel University who joined John Crane in 2013 located in Berkshire, UK. Kanza started her career as an R&D engineer in the division of turbo Gas Seals. She has been responsible for various projects within the realm of new product design and development including patents on turbo Gas Seal technologies.*



*Marwan Jahchan is a Global Dry Gas Seal Manager for the Geo Markets at John Crane and has been working at the company since 2011. Marwan works with the Global John Crane Service Centres to standardise, train and develop them into Super Service Centres. He has 20 years of work experience in engineering where his previous position was Gas Seal R&D Engineer. In this role, he worked on various Dry Gas Seal innovation projects and integrated different sensors to monitor dry gas seal conditions during tests. Marwan holds a BEng (HONS) and is a member of The Institution of Mechanical Engineers.*

## ABSTRACT

Dry gas seals, while ideally non-contacting, must reliably perform under all operating conditions encountered by a compressor, including those conditions which induce contact such as slow roll, turning gear, ratcheting, and windmilling. Windmilling is of concern particularly for compressors driven by aero-derivative turbines, in which the shaft may rotate freely at a relatively low speed, presumably lower than the lift off speed of the gas seal. The critical sealing interface in a dry gas seal must therefore withstand contact without experiencing excessive wear and without degrading the performance of the seal. In an effort to improve the friction and wear-resistance of this interface while in contact, a new material combination was experimentally evaluated: a silicon carbide rotating ring against a stationary ring made of a solid lubricant interspersed within a carbon graphite matrix. The tribological performance of this material combination was assessed via ball-on-disk and full-scale seal tests. The full-scale seal tests were designed to mimic the operating conditions encountered over the life of the seal, comprised of maximum pressures and speeds, numerous start-ups and shut-downs, 20 hours of windmilling, 1000 hours of slow roll, and 37 hours at turbine wash speed. The windmilling speed was run at 90% of the lift off speed of the seal, established through acoustic emission measurements during seal start-ups. This speed presents a challenging scenario for the gas seal as it is running at a relatively high speed while still in contact. After testing, the seal faces exhibited minor wear, with the solid lubricant-doped carbon graphite rings exhibiting the majority of the wear while the harder silicon carbide mating rings remained in excellent condition. Residue matching the carbon graphite material composition was observed on the surface of the silicon carbide ring surface. This material transfer was likely providing a lubricious, protective layer during contacting conditions. Seal leakages were also tracked throughout the test program and found to remain consistent from the beginning to the end of the test program. Dynamic leakages even decreased from the first to the last performance test, indicating that the seal is capable of continued service despite the challenging test program designed to create an “end-of-life” seal condition. Actual leakage values were compared to predicted leakages from a combined CFD and FE model; correlation between the two was quite good for dynamic testing but was off by as much as a factor of ten for static testing. The static leakage discrepancy between the model and measurements is likely caused by manufacturing deviations, whose effect is magnified by the very small film thickness and consequently low leakage during static conditions.

## INTRODUCTION

Historically, dry gas seals for LNG applications have employed a relatively soft stationary ring material against a harder rotating ring material, such as carbon graphite against tungsten carbide or silicon carbide (Shah 1969). An alternative carbon graphite material grade was identified for investigation which is doped with a solid lubricant. The solid lubricant is expected to provide beneficial lubrication when faces are in contact, particularly in dry environments where carbon graphite suffers from increased wear rates (Lancaster 1990). Of all the expected operating conditions of a typical LNG dry gas seal, slow roll (and similarly, turning gear and ratcheting) creates the worst-case wear scenario. The speed during slow roll, turning gear, or ratcheting is sufficiently low to virtually negate the hydrodynamic lift effect of the grooves in the rotating ring, resulting in seal contact. The solid lubricant additive is anticipated to reduce the friction and improve the wear-resistance of the carbon graphite against silicon carbide, thus improving the slow roll performance of the seals.

In order to properly evaluate any new material a comprehensive test methodology needs to be implemented. Possible applications, worst-case scenarios and test complexities were considered to determine a test plan to assess the material at the end-of-life condition of the seal. The new carbon grade was first tested via ball-on-disk tests in dry nitrogen for comparison to the standard grade (without the added solid lubricant) for friction and wear behavior. It was then utilized in full-scale gas seal tests designed to subject the seal to the most severe conditions it could expect to see over its operational life in a compressor. The test program includes performance testing at maximum operational pressure and speed, slow roll testing at low speed for 1000 hours, and several hours at turbine wash speed. In addition, a new test was introduced to evaluate the performance of the seal during “windmilling” of the compressor. Windmilling occurs in certain compressors that are connected to aeroderivative gas turbines, where moving air across the blades causes the shaft to rotate freely while the turbine and compressor are shut down. This was accomplished by running the seal at 90% of its lift off speed. The lift off speed of a seal is the speed at which hydrodynamic lift forces are sufficiently high to separate the seal faces. This windmill test was therefore added to the test program described above, rounding out a rigorous experimental evaluation of the new material combination.

A theoretical model of the seal provided predictions of the contact pressure distribution at the seal interface during slow roll as well as seal leakage estimates at the various test conditions. Comparisons were made between the calculated and measured leakages. Visual inspection and surface traces of the seal wear were also compared to predictions to assess the validity of the computational model.

## BALL-ON-DISK TESTS

Ball-on-disk tests were carried out by a ball-on-disk rig (Anton Paar®) in a dry nitrogen environment. Two different grades of carbon graphite disks were selected for the test: Grade A, the standard carbon graphite formulation, and Grade B, the standard carbon graphite base with a solid lubricant interspersed throughout. The 0.394 in (10 mm) diameter balls were made of silicon carbide (SiC). The applied contact load is 1.12 lbf (5 N).

Figure 1 shows the coefficient of friction (COF) for the two grades of carbon graphite against SiC for the completed test. Grade A carbon against SiC initially exhibited a low COF ( $\sim 0.05$ ), but the friction jumped suddenly to  $\sim 0.6$  after about 200 seconds into the test and continued to fluctuate widely around  $\sim 0.6$  for the remainder of the test. Conversely, grade B maintained a low and stable COF of  $\sim 0.05$  throughout the duration of the test, indicating that grade B offers beneficial lubrication in a dry nitrogen environment.

Post-test surface traces of the wear scars on the carbon disks are provided in Figure 2. Carbon Grade A had a wear scar as deep as 0.0035 in (90  $\mu\text{m}$ ). Meanwhile, carbon Grade B had a wear depth of only 19.7  $\mu\text{m}$  (0.5  $\mu\text{m}$ ).

According to the ball-on-disk test results, the solid lubricant addition to the carbon graphite (Grade B) provides beneficial friction- and wear-reducing behavior in a dry nitrogen environment when compared to the standard carbon graphite alone (Grade A). This material was therefore chosen for further evaluation in a dry gas seal.

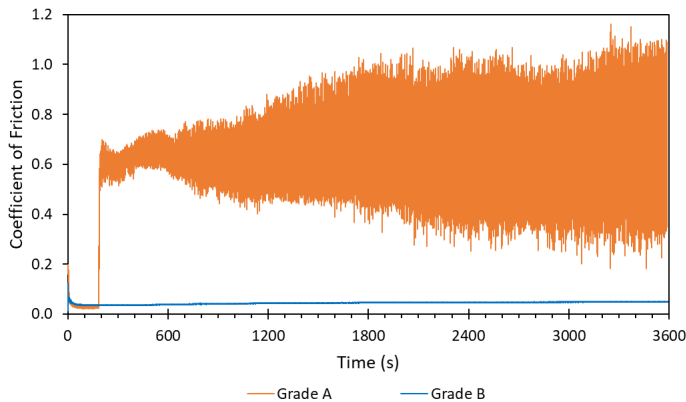


Figure 1. Coefficient of Friction as a Function of Time for Two Carbon Graphite Material Grades.

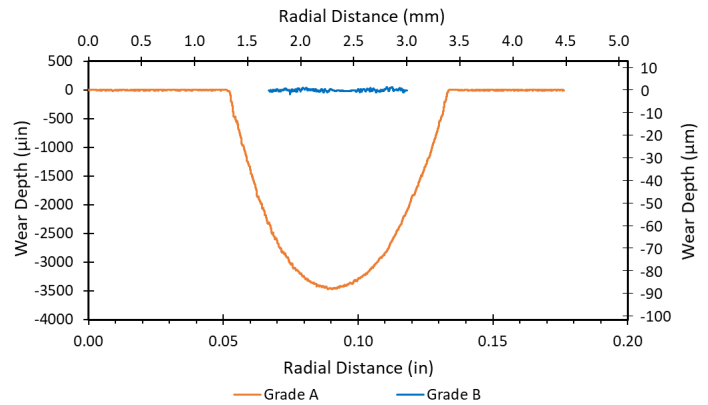


Figure 2. Wear Scar Measurements for Carbon Disks After 1-hour Ball-on-Disk Tests.

## FULL-SCALE GAS SEAL TESTS AND COMPUTATIONAL MODEL

### Gas Seal Configuration

Figure 3 shows a simplified cross section of the tandem seal with arrows indicating the direction of gas flow and the porting used on the test. The tandem seal has two stages: a primary, or inboard (IB) stage, and a secondary, or outboard (OB) stage. Each primary and mating ring pair forms a sealing interface, restricting the gas flow and reducing the pressure from the outer diameter to the inner diameter of the interface. Under normal conditions, the inboard seal interface sees a pressure drop from process pressure at the outer diameter (OD) to near-atmospheric pressure at the inner diameter (ID), while the outboard seal is unpressurized (Stahley 2001). The seal utilized for testing has a balance diameter of 7.374 in (187.3 mm) and bi-directional grooves on the mating ring, allowing for rotation in both the clockwise and counterclockwise directions. Based on the findings from the tribology tests, the mating ring was made of silicon carbide while the primary ring was made of the Grade B carbon graphite interspersed with solid lubricant.

### Test Program

The seals were run according to the following test sequence:

- Initial Performance Test: establishes the baseline leakage performance of the seals up to full operating pressure (827 psig (5.7 MPag)) and speed (6,896 rpm or 222 ft/s (67.6 m/s) surface speed at the balance diameter).
- Windmilling Test: establishes the lift off speed of the seals using acoustic emission (AE) measurements, then assesses the seal's ability to withstand 20 hours of rotation at a speed equal to 90% of the lift off speed.
- Slow Roll Test: subjects the seal to the total cumulative hours of slow roll operation expected over the life of the seal (1000 hours) at slow roll speed (14 rpm or 0.46 ft/s (0.14 m/s) surface speed at the balance diameter), with a 0.08 in (2 mm) axial shift of the shaft every 24 hours to assess the ability of the seal to accommodate axial movement.
- Turbine Wash Test: subjects the seal to 37 hours of turbine wash speed (445 rpm or 14 ft/s (4.4 m/s) surface speed).
- Final Performance Test: measures the leakage performance of the seals after undergoing the above suite of tests (up to full operating pressure and speed) in order to assess the change, if any, in performance from the first test to the last.

The seals were disassembled and inspected between each test to document the condition of the primary and mating ring faces at each stage of testing. Profilometer traces were taken at this time to measure any wear.

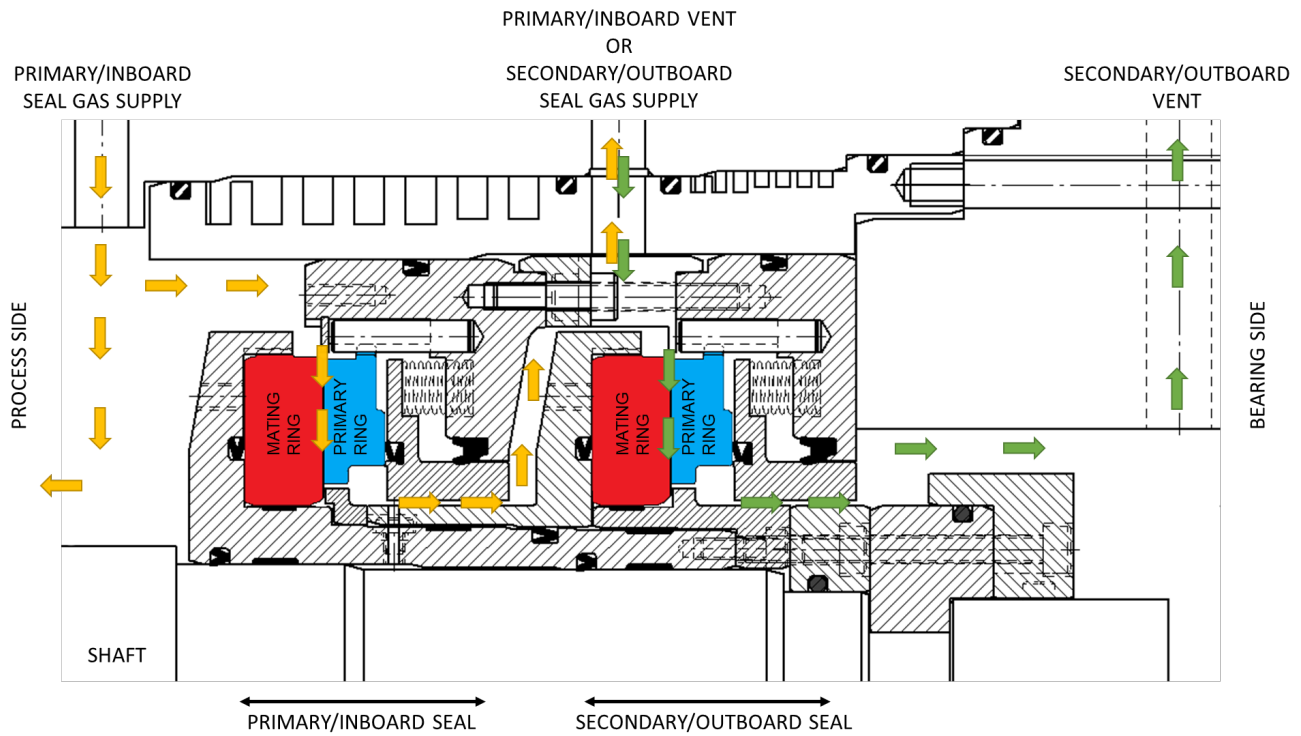


Figure 3. Tandem Gas Seal Cross-Section.

### Test Setup

The seals were tested in a barrel style cell as shown in Figure 4. Two seals were installed at opposite ends of the shaft, mirroring one another to balance the thrust load caused by the internal pressure in the barrel. As each seal is a tandem cartridge with bi-directional grooves, a total of four identical sealing stages were tested in unison. The section view provided in Figure 4 shows the ends of the cell, labeled drive end (DE) near the motor and non-drive end (NDE) opposite the motor, as well as the porting locations used for gas inlets, exits, and instrumentation.

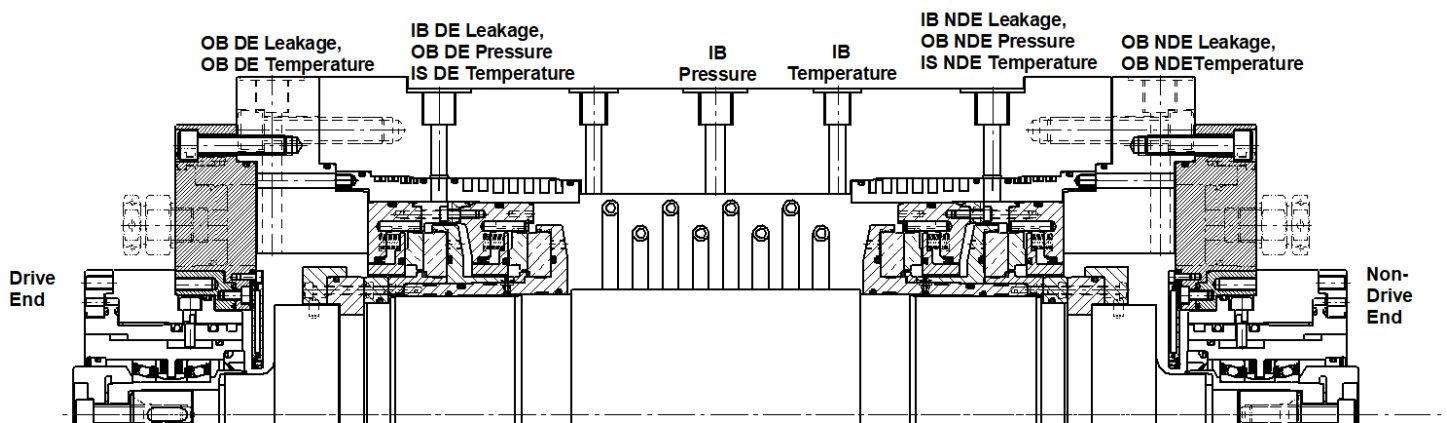


Figure 4. Test Cell Cross-Section with Ports Labeled for Measurement Locations.

The following measurements were recorded during testing:

- Pressure at all seal stages (drive end inboard and outboard, non-drive end inboard and outboard)
- Leakages at all seal stages (drive end inboard and outboard, non-drive end inboard and outboard)
- Gas temperatures at the inboard and inter-stage (IS) spaces
- Primary ring temperatures at the outboard stages (thermocouples were affixed to the backs of the rings)
- Gas dew point
- Shaft axial position
- Motor torque
- Acoustic emissions (AE) on the drive and non-drive ends of the test barrel

An actuator linked to the non-drive end bearing with a travel speed of 0.002 in/s (0.05 mm/s) provided the axial movement of the shaft. During slow roll testing, an axial shift of 0.08 in (2 mm) was performed every 24 hours, alternating directions such that the position of the shaft moved between the +0.04 in (+1mm) and -0.04 in (-1 mm) positions.

Initial and final performance tests used air while the windmilling, slow roll, and turbine wash tests used nitrogen with a dew point of less than -40°F (-40°C).

### Computational Model

Prior to running the seal tests, a combined fluid-solid model was used to predict the seal performance at each of the test conditions. The gas seal model is simplified by considering only the mating and primary rings, which define the sealing interface. The computational model accounts for gas flow, heat transfer, and material deformations of the rings by solving the compressible-flow Reynolds equation coupled with force and energy balance equations, as well as solid mechanics (Lebeck 1991). The calculation of material deformations assumes two-dimensional axisymmetric bodies, while the gas film pressure distribution solved via the Reynolds equation considers the full three-dimensional groove profile.

The coefficient of friction measured by the ball-on-disk testing of 0.05 was used as an input in the seal model, as well as the measured convex surface profiles after lapping. Outputs include the film thickness profile, seal leakage, contact pressure, temperature and stress distributions. Figure 5 shows the predicted deflections and temperatures of the primary and mating rings for the maximum pressure static and dynamic test conditions. The maximum test pressure is 827 psig (5.7 MPag), and the maximum test speed is 6,896 rpm. For the static case, a low speed of 12 rpm was chosen to aid with convergence.

As Figure 5 illustrates, the difference in film thickness between the static and dynamic cases is notable; the minimum film thickness at 6,896 rpm is 3.5X that of the 12 rpm (static) case due to the hydrodynamic lift provided by the grooves at sufficiently high speeds. Note that the interface film thickness is typically on the order of 40-400 μin (1-10 μm). As leakage is proportional to the cube of the film thickness (Lebeck 1991), it follows that the dynamic leakage for this seal is expected to be much higher than the static leakage. The seal leakage at 6,896 rpm is estimated to be ~10X greater than the seal leakage at 12 rpm (static). Furthermore, the gas film has higher axial stiffness dynamically ( $1.39 \times 10^7$  lbf/in ( $2.43 \times 10^9$  N/m)) than statically ( $1.29 \times 10^6$  lbf/in ( $2.25 \times 10^8$  N/m)).

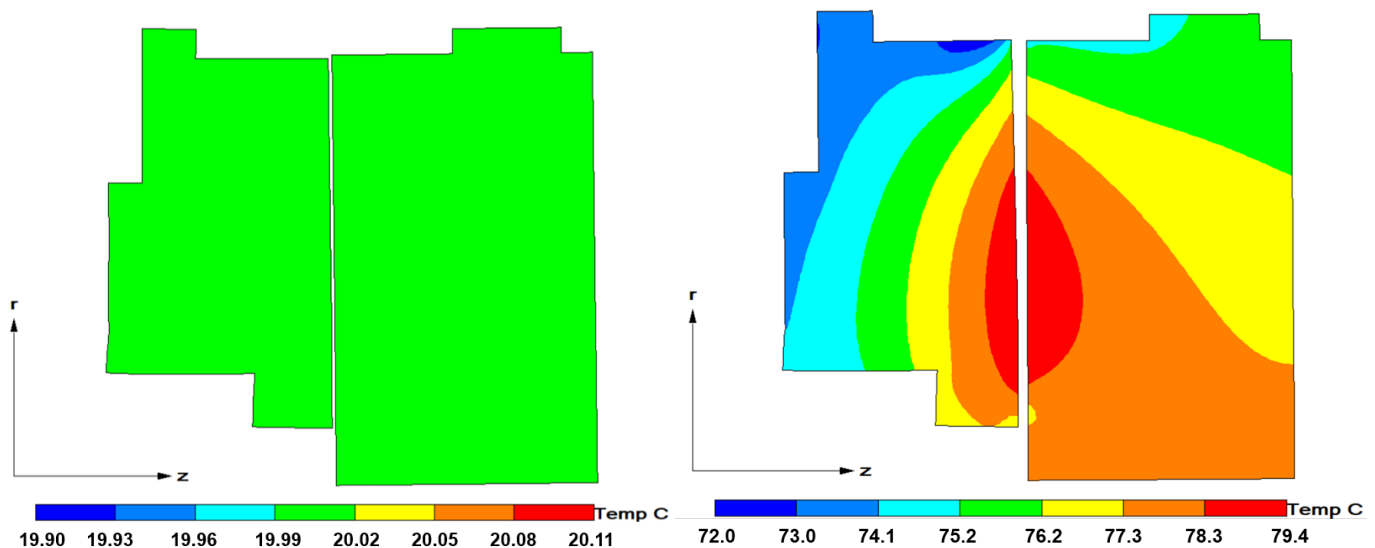


Figure 5. Temperature Distributions and Material Deformations of the Mating and Primary Rings at 827 psig and 12 rpm (Left) and 6,896 rpm (Right). Deformations Are Scaled 200X.

### Test Results

#### Initial Performance Test

The first performance test subjected the seals to a range of pressures and speeds, testing both outboard and inboard seals. Test data of the initial performance test is shown in Figure 6. Note that during outboard pressurization, the inboard pressure was maintained at a higher pressure to avoid reverse pressurization of the inboard seal.

Measured leakage values are normalized by the predicted leakages from the computational model; static leakages are normalized by the predicted leakage at 827 psig (5.7 MPag) and 12 rpm, while dynamic leakages are normalized by the predicted leakage at 827 psig (5.7 MPag) and 6,896 rpm. Static leakages at the inboard seal under maximum pressure initially showed good correlation with the predicted value (normalized leakage  $\approx 1-2$ ). A shift in leakage was observed during the 827 psig (5.7 MPag) hold which was caused by the motor

engaging, followed by some erratic leakages which later stabilized. The split-second spikes in leakage are artificial, caused by the automated switching between the low and high flow meters. The static leakage at the non-drive end outboard seal matched predictions quite well, while the drive end outboard seal leaked higher than predicted. Meanwhile, dynamic leakages for both seals exhibited very good correlation with the calculated value (normalized leakage  $\approx 1$ ).

Static leakages are especially difficult to predict due to the very small film thickness and consequently small leakage. An error of  $<0.03$   $\text{ft}^3/\text{min}$  ( $<1$   $\text{sL}/\text{min}$ ) can be quite large when the seal is leaking very little. As noted above, the dynamic case provides both a higher film thickness and a higher axial stiffness than the static case, which means that manufacturing deviations such as waviness have much less of an effect dynamically than statically.

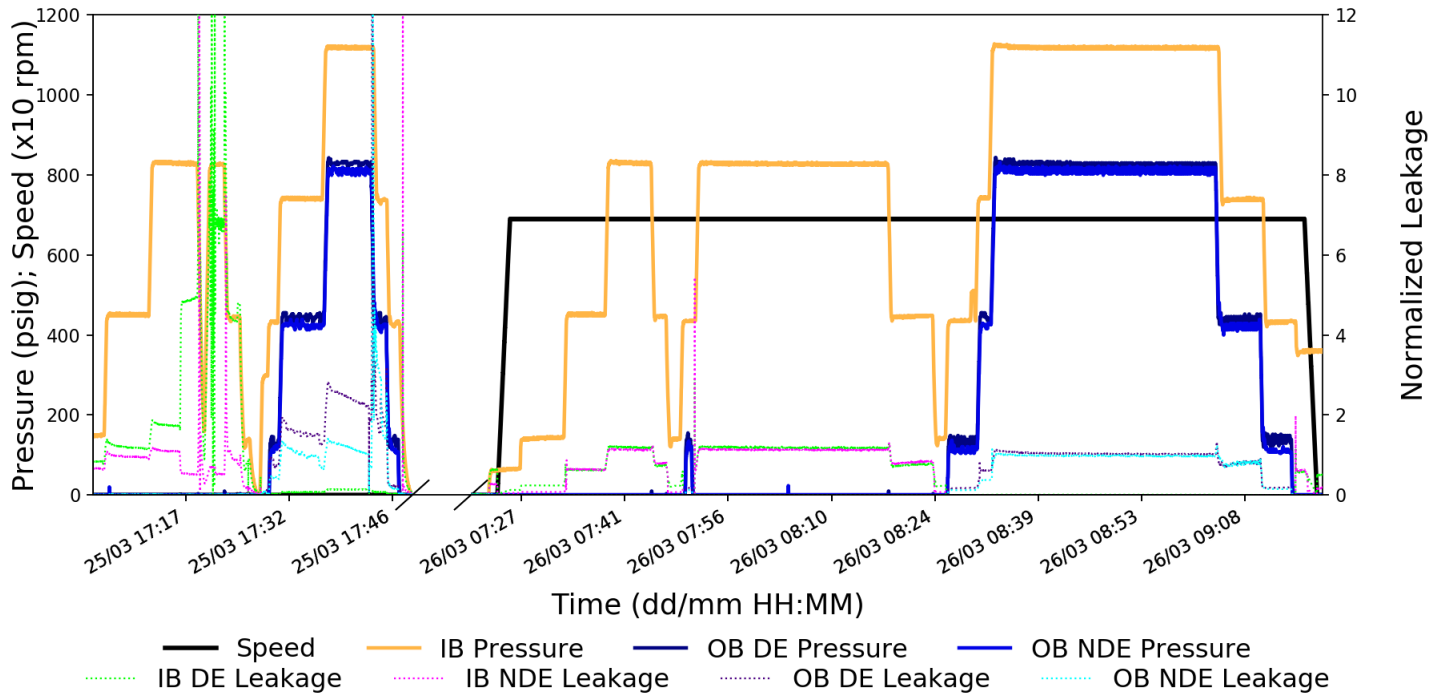


Figure 6. Initial Performance Test Data.

#### Windmilling Test

The seal lift off speed was first measured in order to determine the appropriate speed at which to run the windmilling test. This was accomplished by analyzing the AE signals during speed ramp-ups via multiple consecutive start-stops, as shown in Figure 7. A clear spike in the AE signal is evident during each speed ramp-up, and the speed at which this signal attenuates below a certain threshold is considered the lift off speed. Based on 36 ramp-up events at 146.5 psig (1.0 MPa) with a speed increase rate of 66 rpm/s, the average lift off speed of these seals was determined to be 234 rpm.

Because the purpose of the windmilling test is to run the seal in a relatively high speed yet contacting condition, the target speed is 90% of the seal lift off speed. A low approximation of 200 rpm was chosen as a representative lift off speed, resulting in a windmill test speed of 180 rpm. Targeting the lower end of observed lift off speeds was a conservative approach, as it is more likely to ensure that the seal is in contact during the wind-milling test.

The windmilling test consisted of twenty cycles of 1-hour holds at 180 rpm, with a run up to 3,000 rpm (96.4 ft/s (29.4 m/s) surface speed) in between cycles. Upon completion of the windmill test, the primary and mating ring faces were inspected. Some visible circumferential wear tracks were observed near the inner diameters, as well as a few radially oriented scratches. Dye penetrant was used to confirm that these were surface scratches rather than cracks.

A surface profilometer was utilized to measure the extent of wear on the primary and mating rings. Figure 8 provides a representative trace of the mating ring located at the non-drive end outboard stage. A residue was observed near the inner diameter of the mating rings, which was confirmed by elemental analysis to be the primary ring material (both carbon and the solid lubricant were detected). The first trace shown in green in Figure 8 was taken with the residue still on the surface of the mating ring (before cleaning). This residue was then removed with acetone and the trace (black curve) was remeasured at the same location. As the black curve shows, the wear on the mating rings was quite minimal, measuring less than 1  $\mu\text{m}$  in depth. It was also concentrated near the inner diameter of the rings. This positive result is attributed to the transfer of the soft primary ring material to the mating ring surface; the carbon graphite with solid lubricant formed a protective layer with beneficial lubricating properties.

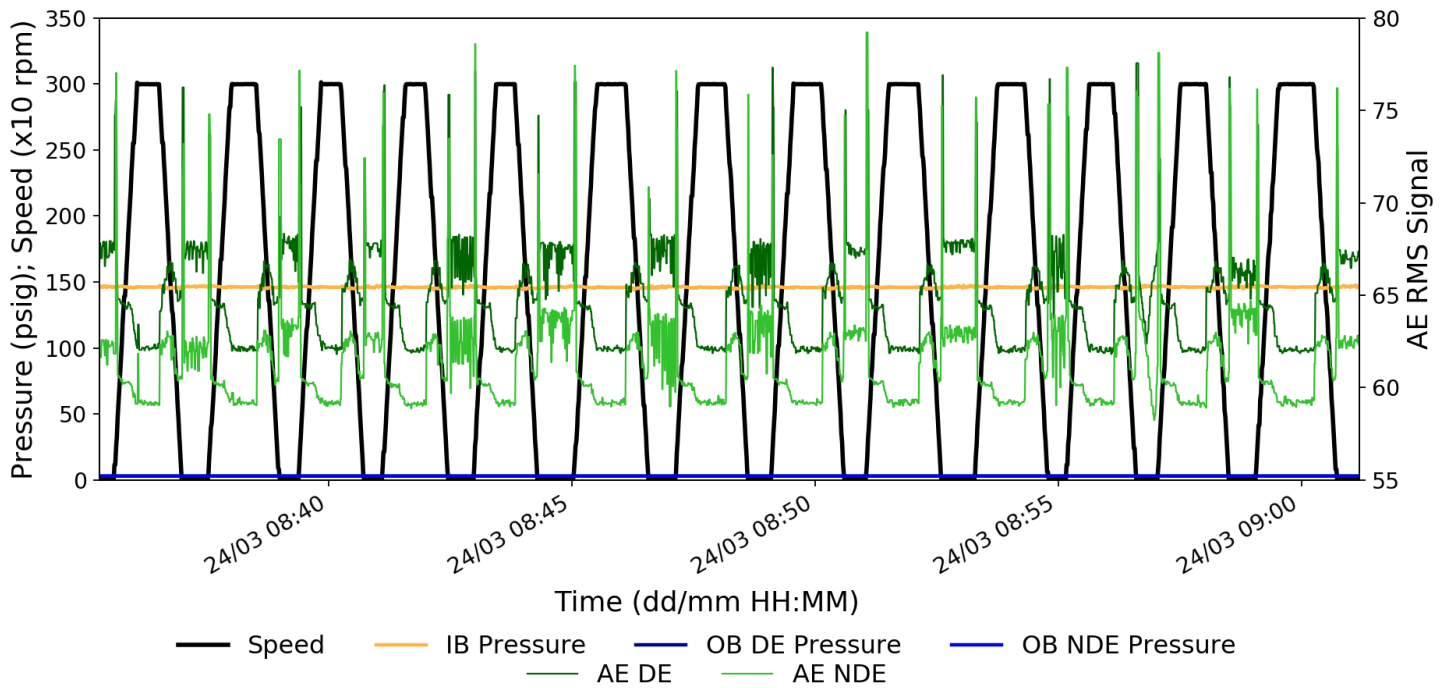


Figure 7. Start-Stop Test Data for Lift Off Speed Calculation.

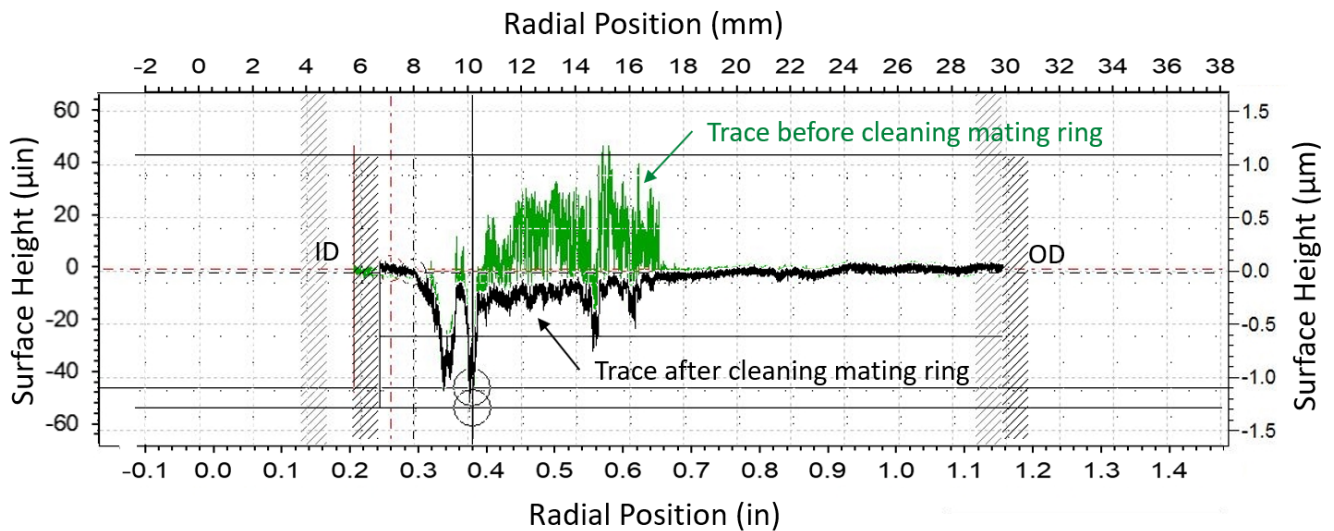


Figure 8. Surface Profile Measurement of the Non-Drive End Outboard Mating Ring After the Windmilling Test.

*Slow Roll Test*

Slow roll testing subjected the seals to 1000 total hours of slow roll at 14 rpm. Once every 24 hours, the seals were run at 3,000 rpm for 15 minutes and the axial position of the seal was shifted to  $\pm 0.04$  in (1 mm) from center. The complete slow roll test data is provided in Figure 9. Temperatures around the seal and the nitrogen dew point cycled daily with ambient temperature fluctuations. Seal temperatures also increased temporarily during the high-speed runs but returned to a normal range of approximately 50-86°F (10-30°C) throughout the holds at 14 rpm. The daily axial shift did not have a noticeable effect on the leakages, indicating the seals ability to accommodate axial movement.

The drive end inboard seal was leaking approximately 3 times higher than the non-drive end seal, although the actual magnitude of the leakages was very low for both seals  $< 0.14$  sft<sup>3</sup>/min ( $< 4$  sL/min). Leakage values plotted in Figure 9 are normalized by the predicted leakage of nitrogen at the slow roll conditions (146.5 psig (1.0 MPag), 14 rpm, and 68°F (20°C)), and were approximately 10-30 times

higher than calculated by the seal model. The rotational speed during slow roll is so low that the seal is in a near-static state, so accurate correlation of predictions to actual leakage values is difficult to obtain due to the reasons discussed previously.

In general, the AE signals remained low throughout the slow roll cycles. However, there were some periods of high AE activity, most notably from May 15-16 and the final two days of testing (the high AE signals on the first day were likely artificial, as the probe connections and groundings were being adjusted at that time). These could have been caused by debris passing through the seal, by prolonged seal face contact, or by external noise from the test rig area. If the seals had been in a state of prolonged, heavy contact, an accompanying increase in temperature would have been expected, which was not observed.

Immediately following the slow roll test, the seal faces were inspected. Images of the primary and mating ring faces are shown in Table 1. Primary and mating ring surface profile measurements are presented in Table 2. Comparing both the pictures and profile measurements of the primary rings, there appeared to be a small increase in the wear band near the inner diameter, but no significant damage caused by the 1000 hours of slow roll. The drive end inboard traces before and after the slow roll test were nearly identical. The drive end outboard and non-drive end inboard primary rings showed a slight increase in material removal and wear tracks near the inner diameter, but very minor; the magnitude of the wear scars was less than about 400  $\mu\text{in}$  (10  $\mu\text{m}$ ). The non-drive end outboard stage does show a single new 0.001 in (30  $\mu\text{m}$ ) wear scar near the mid diameter but otherwise looks quite similar to its condition prior to the slow roll test. On all four mating rings, the measured wear was less than 79  $\mu\text{in}$  (2  $\mu\text{m}$ ) deep. When compared to the < 39  $\mu\text{in}$  (1  $\mu\text{m}$ ) wear scar measured after the windmill test, the mating rings experienced almost no additional damage as a result of 1000 hours of slow roll testing.

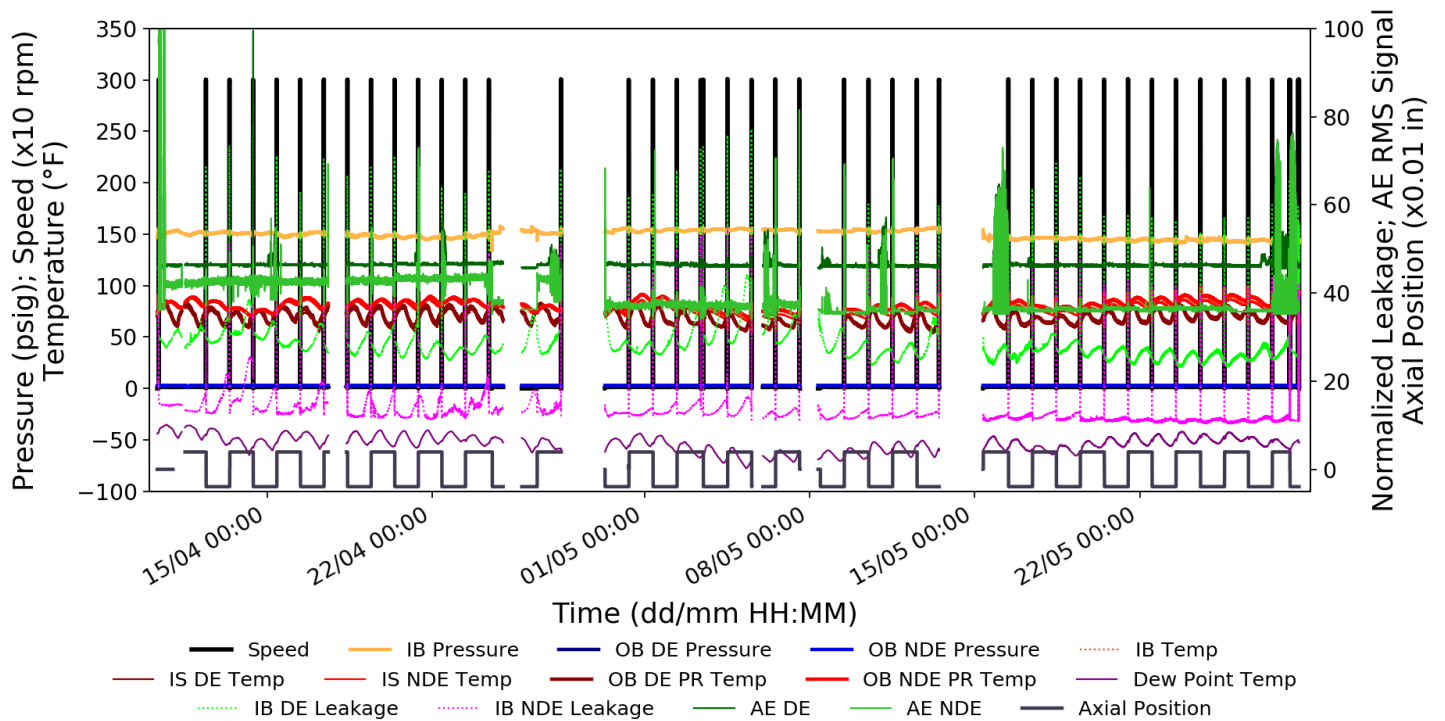


Figure 9. Slow Roll Test Data.



Table 1. Seal Face Condition Before and After the Slow Roll Test.

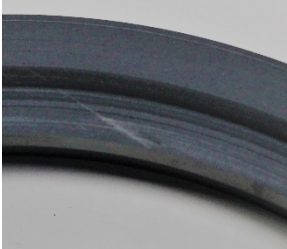



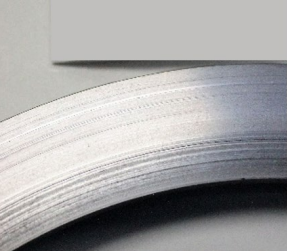


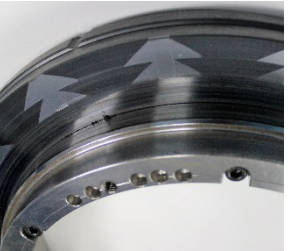




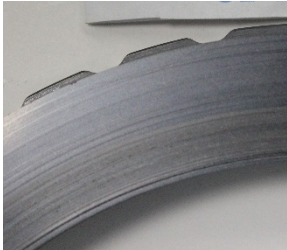



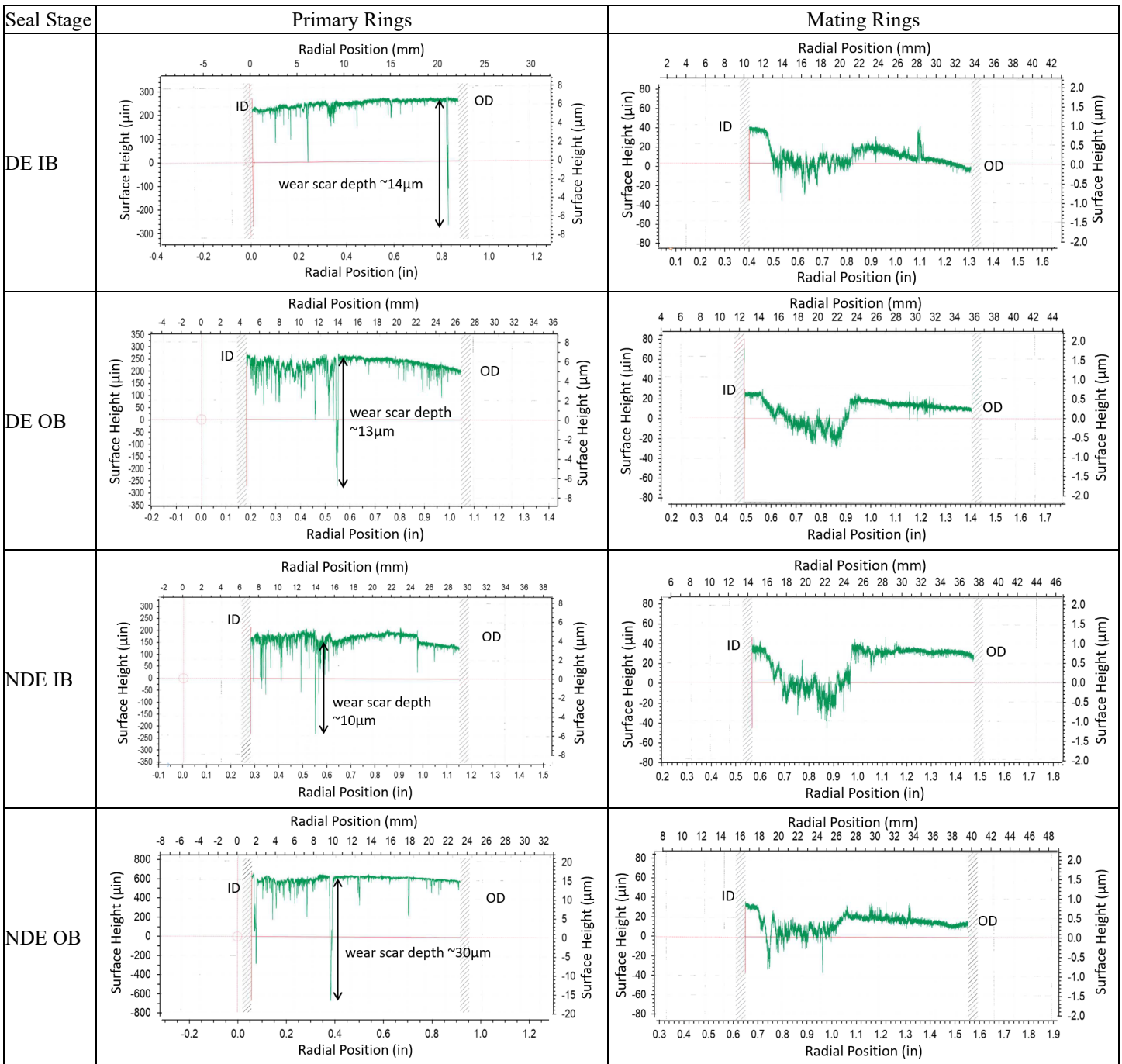
Seal Stage	Before Slow Roll Test		After Slow Roll Test	
DE IB				
DE OB				
NDE IB				
NDE OB				

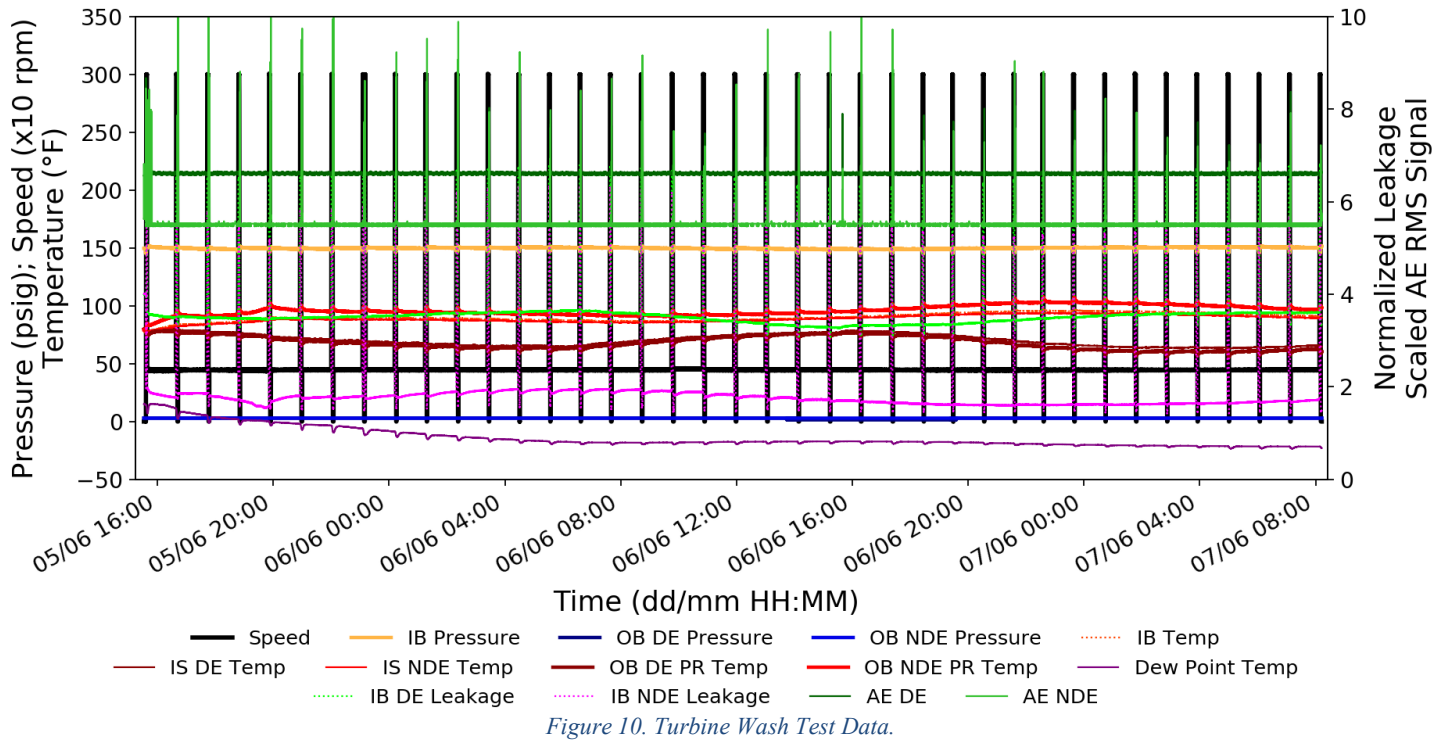
Table 2. Primary and Mating Ring Surface Profile Measurements Taken After the Slow Roll Test.



**Turbine Wash Test**

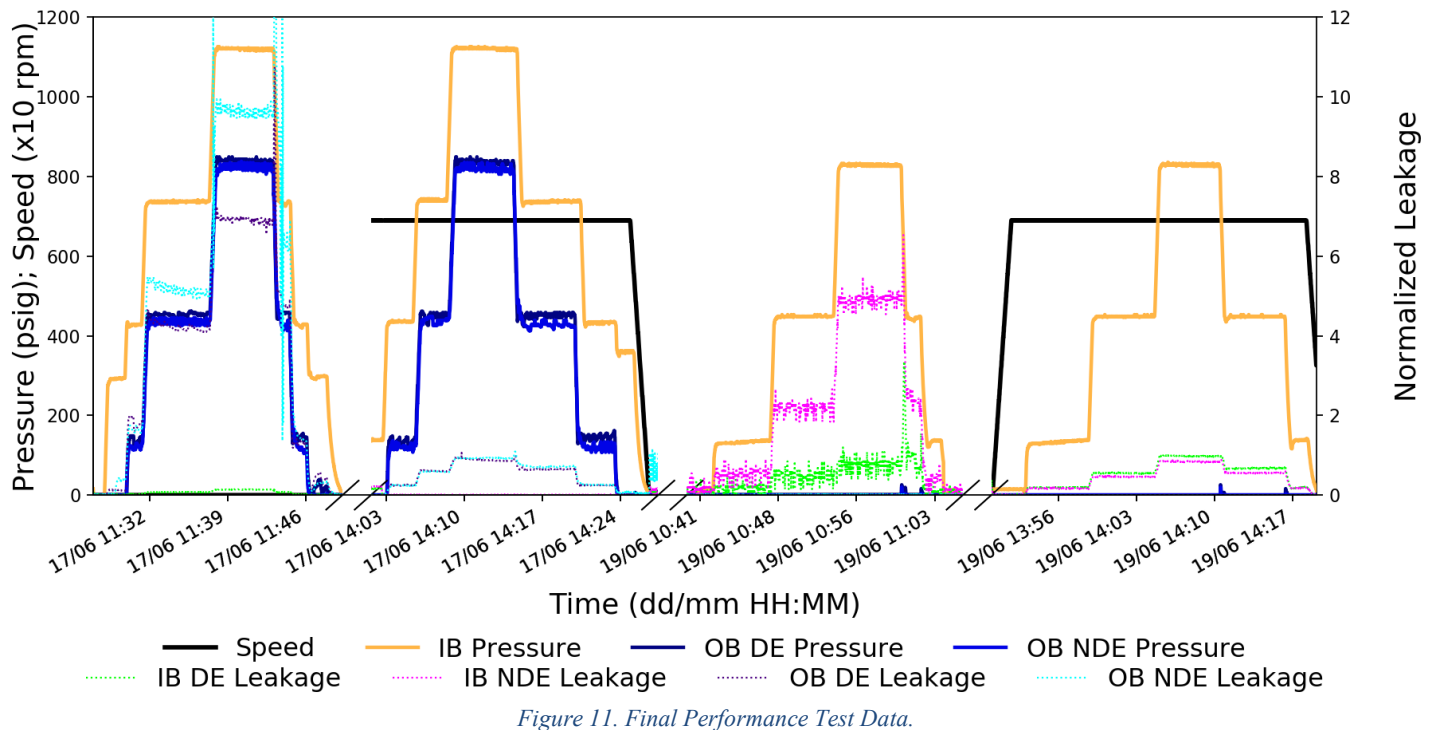
After slow roll testing, the seals were subjected to a turbine wash test of 37 one-hour runs at 445 rpm with 15 minutes at 3,000 rpm in between. Test data is shown in Figure 10. Leakages are normalized by the computational model predictions at 445 rpm and 146.5 psig (1.0 MPag) inboard pressure. Actual leakages were approximately 1.5 to 4 times the predicted leakages.

The measured AE remained low throughout the 445 rpm holds and exhibited characteristic lift off and touch down spikes while ramping up in speed and coasting down in speed, respectively. These observations indicate that the seal was lifted off (*i.e.*, not contacting) while running at the turbine wash speed. This is expected given the lower lift off speeds measured in previous tests.



#### Final Performance Test

The seals were tested once again to the maximum operating pressure and speed conditions. Test data for the final performance test is provided in Figure 11. As before, the static and dynamic leakages were normalized by predicted leakages at maximum pressure and their respective speeds. Similar to the initial performance test, the dynamic leakages at 827 psig (5.7 MPag) showed excellent correlation with predictions. Statically, the actual leakages were up to 10 times higher than predicted values. As previously noted, this discrepancy at static conditions is likely due to a combination of manufacturing deviations, the very small film thickness, and the consequently small predicted leakage.



The primary reason for running the final performance test was to assess the seal behavior, and more specifically leakages, after the seal

had been through enough testing to represent an “end-of-life” condition. To this end, average leakages from the first and last performance tests are compared in Figure 12. The static leakages increased in three of four seal stages, particularly for the two outboard stages. However, all leakages remained well below the guaranteed static limit. Dynamically, the seal leakages remained very similar from the initial to the final test, and slightly decreased across all four stages. Again, these leakages were all substantially below the guaranteed dynamic limit as shown on the graph. These results demonstrate that the seal is still operational after 1000 hours of cumulative slow roll, 20 hours of windmilling, 37 hours of turbine wash, and over 100 start-ups and shut-downs.

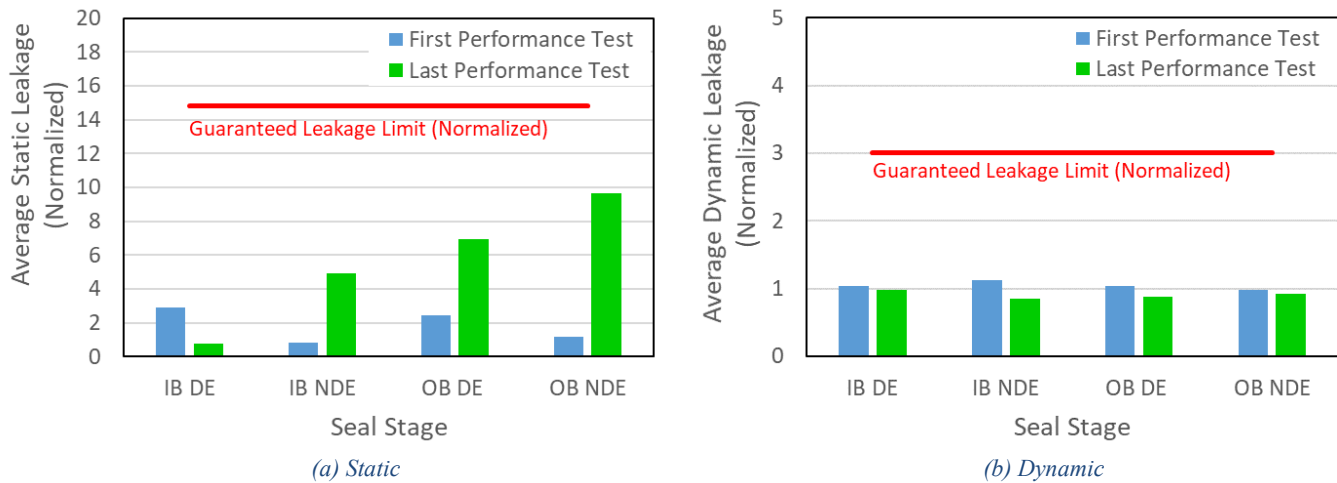


Figure 12. Average Leakage Comparisons from First and Last Performance Tests for (a) Static and (b) Dynamic Pressurization at 827 psig (5.7 MPag).

The condition of the primary and mating ring surfaces after the final performance test is shown in Table 3. The drive end primary ring has a scratch near the outer diameter which did not occur during the final performance test (the scratch was noted while preparing the seal for the final test and likely occurred either during seal handling or torque measurements). Fortunately, the leakage data demonstrates that the accidental scratch on the drive end inboard primary ring did not adversely affect the performance of the seal. Barring this scratch, the condition of the primary and mating rings is the same as that after the slow roll test; the seal faces did not experience any discernable increase in wear as a result of the turbine wash or final performance tests as measured by surface profilometer traces. While the primary rings did wear slightly during the slow roll and windmilling tests due to the contacting conditions, they continued to perform well as sealing surfaces. For the mating rings in particular, the final maximum measured wear depth was approximately 79  $\mu\text{in}$  (2  $\mu\text{m}$ ), but generally even less across all seal stages. The primary rings, as the softer material with the lubricious solid lubricant deposited throughout the carbon matrix, protected the hard SiC mating rings.

## CONCLUSIONS


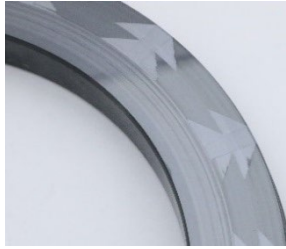






Utilizing ball-on-disk testing with a controlled environment, two carbon graphite material grades were evaluated for tribological performance in dry nitrogen. A carbon graphite grade with interspersed solid lubricant was selected for further testing in a dry gas seal due to its excellent friction and wear resistance.

After completing over 1060 hours of testing at various speeds and pressures, including over 100 start-ups and shut-downs, minimal wear was observed on the SiC mating ring surfaces. Although the softer primary rings, made of carbon graphite with solid lubricant, exhibited slightly more wear, it was likely providing a protective layer over the SiC during contacting conditions, as evidenced by the carbon and solid lubricant residue observed on the mating ring surface. Furthermore, having the solid lubricant distributed throughout the carbon graphite ring allows for continued beneficial friction reduction at the interface even after wear occurs. As expected, the low-speed tests, namely windmilling and slow roll, accounted for the majority of wear observed on the seal rings. However, the seal leakages remained consistent between the first and last performance tests, especially dynamically.

A 2D, axisymmetric seal model provided estimates of the leakage and contact conditions under various test conditions. Calculated leakages at high speeds matched well to values measured during tests. However, static leakages were difficult to accurately model due to small film thicknesses, which are much more sensitive to minor part deviations such as waviness.

The functional condition of these seals at the end of testing demonstrates that the new material combination is a viable solution for gas seals in dry nitrogen applications which are subjected to prolonged periods of low speed or are likely to experience seal face contact. Additional testing that would complement this work should include tests within other gas environments to determine the suitability of this material combination for other applications.

Table 3. Seal Face Condition After the Final Performance Test.

Seal Stage	After Final Performance Test	
DE IB		
DE OB		
NDE IB		
NDE OB		

## **NOMENCLATURE**

COF	= Coefficient of friction
DE	= Drive end (of the test barrel, near the motor)
IB	= Inboard (or primary) seal stage in a tandem seal
ID	= Inner diameter
MR	= Mating (rotating) ring
NDE	= Non-drive end (of the test barrel, opposite the motor)
OB	= Outboard (or primary) seal stage in a tandem seal
OD	= Outer diameter
OEM	= Original equipment manufacturer
PR	= Primary (stationary) ring
SiC	= Silicon carbide

## **REFERENCES**

- Lancaster, J. K., 1990, A Review of the Influence of Environmental Humidity and Water on Friction, Lubrication, and Wear, *Tribology International*, 23, 6, pp. 371-389.
- Lebeck, A. O., 1991, *Principles and Design of Mechanical Face Seals*, New York, New York: John Wiley & Sons, Inc.
- Shah, P., 1969, Dry Gas Compressor Seals, Proceedings of the 17<sup>th</sup> Turbomachinery Symposium, Turbomachinery Laboratory, Texas A&M University, College Station, Texas, pp. 133-140.
- Stahley, J. S., 2001, Design, Operation, and Maintenance Considerations for Improved Dry Gas Seal Reliability in Centrifugal Compressors, Proceedings of the 30<sup>th</sup> Turbomachinery Symposium, Turbomachinery Laboratory, Texas A&M University, College Station, Texas, pp. 203-208.

## **ACKNOWLEDGEMENTS**

The authors would like to thank Aaron Date for assistance with testing, and Jorge Pacheco and Simon Elcock for technical guidance.